

Topics in Applied Physics 139

David J. Lockwood  
Lorenzo Pavesi *Editors*

# Silicon Photonics IV

Innovative Frontiers

 Springer

# **Topics in Applied Physics**

Volume 139

## **Series Editors**

Young Pak Lee, Physics, Hanyang University, Seoul, Korea (Republic of)

David J. Lockwood, Metrology Research Center, National Research Council of Canada, Ottawa, ON, Canada

Paolo M. Ossi, NEMAS - WIBIDI Lab, Politecnico di Milano, Milano, Italy

Kaoru Yamanouchi, Department of Chemistry, The University of Tokyo, Tokyo, Japan

Topics in Applied Physics is a well-established series of review books, each of which presents a comprehensive survey of a selected topic within the domain of applied physics. Since 1973 it has served a broad readership across academia and industry, providing both newcomers and seasoned scholars easy but comprehensive access to the state of the art of a number of diverse research topics.

Edited and written by leading international scientists, each volume contains high-quality review contributions, extending from an introduction to the subject right up to the frontiers of contemporary research.

Topics in Applied Physics strives to provide its readership with a diverse and interdisciplinary collection of some of the most current topics across the full spectrum of applied physics research, including but not limited to:

- Quantum computation and information
- Photonics, optoelectronics and device physics
- Nanoscale science and technology
- Ultrafast physics
- Microscopy and advanced imaging
- Biomaterials and biophysics
- Liquids and soft matter
- Materials for energy
- Geophysics
- Computational physics and numerical methods
- Interdisciplinary physics and engineering

We welcome any suggestions for topics coming from the community of applied physicists, no matter what the field, and encourage prospective book editors to approach us with ideas. Potential authors who wish to submit a book proposal should contact Zach Evenson, Publishing Editor:

[zachary.evenson@springer.com](mailto:zachary.evenson@springer.com)

Topics in Applied Physics is included in Web of Science (2019 Impact Factor: 0.633), and is indexed by Scopus.

More information about this series at <http://www.springer.com/series/560>

David J. Lockwood · Lorenzo Pavesi  
Editors

# Silicon Photonics IV

Innovative Frontiers

 Springer

*Editors*

David J. Lockwood  
National Research Council of Canada  
Metrology Research Centre  
Ottawa, ON, Canada

Lorenzo Pavesi  
Department of Physics  
University of Trento  
Povo, Italy

ISSN 0303-4216

ISSN 1437-0859 (electronic)

Topics in Applied Physics

ISBN 978-3-030-68221-7

ISBN 978-3-030-68222-4 (eBook)

<https://doi.org/10.1007/978-3-030-68222-4>

© The Editor(s) (if applicable) and The Author(s), under exclusive license to Springer Nature Switzerland AG 2021

This work is subject to copyright. All rights are solely and exclusively licensed by the Publisher, whether the whole or part of the material is concerned, specifically the rights of translation, reprinting, reuse of illustrations, recitation, broadcasting, reproduction on microfilms or in any other physical way, and transmission or information storage and retrieval, electronic adaptation, computer software, or by similar or dissimilar methodology now known or hereafter developed.

The use of general descriptive names, registered names, trademarks, service marks, etc. in this publication does not imply, even in the absence of a specific statement, that such names are exempt from the relevant protective laws and regulations and therefore free for general use.

The publisher, the authors and the editors are safe to assume that the advice and information in this book are believed to be true and accurate at the date of publication. Neither the publisher nor the authors or the editors give a warranty, expressed or implied, with respect to the material contained herein or for any errors or omissions that may have been made. The publisher remains neutral with regard to jurisdictional claims in published maps and institutional affiliations.

This Springer imprint is published by the registered company Springer Nature Switzerland AG  
The registered company address is: Gewerbestrasse 11, 6330 Cham, Switzerland

# Preface

After 20 years of development, silicon photonics has reached commercial maturity with many available products. From 2020 to 2025, predicted growth rates of the associated market are in excess of 20% for conservative estimates to more than 30% for more optimistic estimates. In addition to Datacom and Telecom, many other applications are entering the silicon photonic products market. Particularly promising are the applications in the healthcare sector and in the automotive sector where high-quality and low-cost silicon photonic sensors, laser ranging systems and detectors allow a pervasive penetration of the technology. From the very start of silicon photonics, we follow its blossoming development from basic science to engineering and technology via a series of books entitled *Silicon Photonics*, all published by Springer in their *Topics in Applied Physics* series. The original intention, when the first book was published, was to underline the update to silicon electronics through the use of photons, which avoids the bottlenecks created with electrons for information exchange (interconnection bottleneck). *Silicon Photonics I* was based on the underlying fundamental research that was needed to bring these concepts into reality. Volume II of the series, then, covered the burgeoning applications scenario, and *Silicon Photonics III* provided overviews of practical applications of this technology in industry. Luckily, the field of silicon photonics is still presenting many interesting developments spanning from fundamental research where the use of new materials enables novel functionalities in silicon to the development of new technologies and computation paradigms where silicon photonics is making the difference. We feel the time is right to discuss these recent progresses to encompass the widening interest in the use of silicon photonics.

This fourth book in the series on silicon photonics gathers in-depth discussions of recent advances that go beyond already established and applied concepts. The chapters provided in this book by experts in their fields cover not only new research into the highly desired goal of light production in Group IV materials, but also change in the principles driving the development of integrated circuits, novel measurement strategies and novel technologies. Finally, the new paradigms in information processing and telecommunication are covered with the claim that silicon photonics is a proper platform for their realization.

Chapters in the first part of the book on *Advances in Fundamental Research* review recent progresses in the enduring search for crystalline-silicon-compatible light emitters and innovative applications of silicon photonics. For two decades now, there has been intensive research into overcoming the difficulty of obtaining efficient light emission from Si and Ge due to their indirect band gaps. In the past, various methods of inducing a direct gap have been introduced and lasing action has been observed in both Si and Ge, but so far, the performance at room temperature has not been good enough to produce the desired CMOS compatible room temperature laser. Recent work has shown that strained nanostructures of Group IV materials are the most promising candidates for room temperature lasers, as shown for Si in Chap. 1 by Kateřina Dohnalová and Kateřina Kůsová, for disordered Ge in Chap. 2 by Moritz Brehm, for GeSn and SiGeSn alloys in Chap. 3 by Vincent Reboud et al., and crystalline Ge in Chap. 4 by Nelson L. Rowell and David J. Lockwood. In Chap. 5, Simone Rossi, Elisa Vitiello and Fabio Pezzoli demonstrate that Ge-based heterostructures offer innovative solutions to the challenges of integrating spin functionalities into silicon photonics.

Chapters in the second part of the book on *Advances in Integration Architectures* review novel concepts and recent progress in the design of integrated photonic circuits for, and diverse applications of, silicon photonics. In Chap. 6, Hon Ki Tsang et al. introduce some of the numerous applications of subwavelength grating structures employed within silicon photonics devices. Subwavelength gratings have attracted interest recently, as they provide a useful degree of freedom for the crafting of the effective refractive index of the material incorporated in photonic devices. The implementation of quantum mechanics has been the driving force of the most intriguing designs of photonic structures. Non-Hermitian physics, which breaks the conventional scope of quantum mechanics based on the Hermitian Hamiltonian, has been widely explored in the silicon photonics platform, with promising new designs involving the refractive index, modal coupling and gain-loss distribution. In Chap. 7, Changqing Wang, Zhoutian Fu and Lan Yang explore the merger of the non-hermitian physics and classical silicon platforms. Topological photonic insulators have attracted considerable attention due to their unique ability to transport light via topologically protected edge states that are immune to defect scattering so that engineering of robust photonic devices that are insensitive to fabrication imperfections is made possible. Chapter 8 comprises a review by Shirin Afzal, Tyler James Zimmerling and Vien Van of the key concepts of topological insulator systems in one and two dimensions and their practical realization using coupled microring resonator lattices. In Chap. 9, Scott Jordon presents a new parallel digital gradient search technique for rapid automated alignment of devices on silicon photonics integrated circuits. Such a production tool is badly needed now owing to the increasing complexity of silicon photonics integrated circuits.

Chapters in the third part of the book on *Advances in Computation Schemes* review paradigm changing architectures where recent progress in silicon photonics enables new computer technology. In Chap. 10, Bicky A. Marquez et al. report

on neuromorphic architectures on silicon photonics platforms, which enable high-bandwidth, low-latency, low-energy applications. Neuromorphic photonics implements the machine learning methodology in integrated photonics. It exploits the advantages of optics, including the ease of analog processing and full parallelism achieved at the speed of light by employing multiple signals in a single waveguide. Due to its mature semiconductor fabrication processes and the capability to integrate large quantum photonic circuits on a single device, silicon quantum photonics is emerging as a promising platform to develop photonic quantum processor chips. In Chap. 11, Stefano Paesani and Anthony Laing review recent results in developing key building blocks for chip-scale photonic quantum devices and deliberate on progress made toward useful large-scale quantum photonic computers. Finally, in Chap. 12, Marco Fiorentino et al. discuss recent progress toward an open silicon photonics ecosystem targeted at computer applications where there is now an urgent need for standardized industrial production systems.

We hope that the readers will share our enthusiasm about this book, which shows the healthy status of silicon photonics despite the difficulties given by the present situation. We thank all the authors of the present volume for their invaluable contributions, especially considering the extensive restrictions in their work arena resulting from the COVID-19 global pandemic. At the same time, we are grateful to the editorial and production staff of Springer Nature for their support, patience and professional editing. Last but not least, we are indebted to our co-workers who are the real driving force behind our work. They do share with us their research, passion and, mostly importantly, friendship.

Ottawa, Canada  
Trento, Italy  
December 2020

David J. Lockwood  
Lorenzo Pavesi



# Contents

## Part I Advances in Fundamental Research

<b>1</b>	<b>Optical Properties of Si Nanocrystals Enhanced by Ligands</b>	<b>3</b>
	Kateřina Dohnalová and Kateřina Kůsová	
1.1	Introduction	4
1.1.1	Quantum Confinement	5
1.1.2	Complex Role of Surface Chemistry	7
1.1.3	The <i>K</i> -Space Projections of the Density of States	13
1.2	Fast Radiative Rate in Hydrogen- and Oxide-Capped Silicon Nanocrystals	17
1.2.1	Oxidation of Hydrogen-Terminated Silicon Nanocrystals	17
1.2.2	Emergence of the F-Band in Oxidized Si-NC	18
1.2.3	Silica Defects	20
1.2.4	Role of Nitrogen	23
1.3	Organically Coated Si-NCs with a Fast Emission Rate	25
1.3.1	Single-Dot Spectroscopy of Si-NCs with Fast Radiative Rates	27
1.3.2	Enhanced Radiative Rate Measured by Drexhage Experiment	31
1.4	Theoretical Simulations of Si-NCs with Ligands	33
1.4.1	Role of an Electronegative Ligand/Environment	34
1.4.2	Role of Tensile Strain	37
1.4.3	Interplay Between the Charge Transfer and Tensile Strain	40
1.4.4	Thermal Population of States	46
1.5	Summary and Outlooks	50
	References	53
<b>2</b>	<b>Light-Emission from Ion-Implanted Group-IV Nanostructures</b>	<b>67</b>
	Moritz Brehm	
2.1	Introduction to the Chapter	68

2.1.1	Background .....	69
2.1.2	In a Nutshell: Potential Light Sources for Si Photonics .....	70
2.1.3	All-Group-IV Approaches .....	71
2.1.4	Group-III-V on Group-IV Approaches .....	72
2.2	Epitaxial Group-IV Nanostructures on Silicon .....	75
2.3	Ion Implantation into Ge Quantum Dots on Silicon .....	80
2.3.1	DEQD Fabrication Procedure .....	82
2.3.2	Light-Emission from DEQDs .....	85
2.3.3	Considerations Toward Large-Scale Integration Possibilities .....	89
2.3.4	Electrical Injection .....	89
2.3.5	Scalability of DEQD Densities .....	92
2.3.6	Thermal Budget and Annealing of DEQDs .....	94
2.3.7	Curing and Passivation of Non-radiative Recombination Centers .....	96
2.4	Summary and Future Directions in DEQD Research .....	98
	References .....	99
<b>3</b>	<b>Lasing in Group-IV Materials .....</b>	<b>105</b>
	V. Reboud, D. Buca, H. Sigg, J. M. Hartmann, Z. Ikonik, N. Pauc, V. Calvo, P. Rodriguez, and A. Chelnokov	
3.1	Introduction .....	107
3.2	Fabrication: Ge-Based Epitaxy and Processes for Group-IV Indirect and Direct Bandgap Material .....	109
3.2.1	Germanium Growth .....	109
3.2.2	Germanium Tin Growth .....	114
3.2.3	Ge-Based Materials Processing .....	121
3.2.4	Electrical Contacts on Ge-Based Materials: A Focus on GeSn .....	125
3.3	Effects of Strain and Sn for Bandstructure Manipulation .....	129
3.3.1	Strain Control in Germanium-Based Materials .....	129
3.3.2	Band Structures and Band Alignment .....	135
3.3.3	Gain Calculation of Strained Ge-Based Materials (Ge, GeSn, SiGeSn) .....	142
3.4	Group-IV Lasing .....	145
3.4.1	Optical Cavity Design .....	148
3.4.2	Lasing in Ge .....	153
3.4.3	Lasing in GeSn .....	156
3.5	Optoelectronic Devices .....	168
3.5.1	Photodetectors .....	168
3.5.2	Electrically Pumped Devices .....	173
3.6	Outlook and Conclusion .....	178
	References .....	180

<b>4</b>	<b>Light Emission from Germanium Nanostructures</b>	<b>197</b>
	Nelson L. Rowell and David J. Lockwood	
4.1	Introduction	197
4.2	Optical Properties of Bulk Ge	198
4.2.1	Band Structure	198
4.2.2	Absorption	199
4.2.3	Temperature Dependence—Ge Energy Gap	200
4.2.4	Stress	201
4.2.5	Optical Emission from Bulk Ge	202
4.3	Developments with Ge for Photonic Emitters	204
4.4	Optical Emission from Ge Nanocrystals	205
4.4.1	Outline	205
4.4.2	Photoluminescence (PL) Measurements	205
4.4.3	Ge Quantum Dot Ensembles	208
4.4.4	Self-organized Ge Nanocrystals (NCs)	212
4.5	Prospects for CMOS Compatible Devices	232
	References	233
<b>5</b>	<b>Optical Spin Orientation in Ge-Based Heterostructures</b>	<b>237</b>
	Simone Rossi, Elisa Vitiello, and Fabio Pezzoli	
5.1	Introduction	237
5.1.1	A Minimal Guide to Optical Spin Orientation	237
5.2	Bulk Ge	246
5.2.1	Energy Relaxation and Spin Dynamics	248
5.2.2	Spin Lifetime	253
5.3	Ge Heterostructures	259
5.3.1	Strained Ge Epilayer	259
5.3.2	Quantum Confined Heterostructures: Ge/SiGe Quantum Wells	262
5.4	Alloying Ge with Sn	268
5.4.1	Spin Relaxation and Spin Dephasing Time in GeSn	269
5.5	Future Perspective	271
5.5.1	Spin Photodiode and Spin-LEDs	272
5.5.2	Spin-Charge Interconversion Phenomena	273
5.6	Conclusion	276
	References	277
<b>Part II Advances in Integration Architectures</b>		
<b>6</b>	<b>Subwavelength Silicon Photonics</b>	<b>285</b>
	Hon Ki Tsang, Xia Chen, Zhenzhou Cheng, Wen Zhou, and Yeyu Tong	
6.1	Introduction	286
6.2	Effective Medium Theory	287
6.2.1	Rytovs’s Equations and Application in Periodic Dielectric Subwavelength Gratings	287
6.2.2	Spectral Range of Validity of EMT	290

6.3	Subwavelength Waveguide Grating Couplers .....	291
6.3.1	Introduction .....	292
6.3.2	A Brief Review .....	293
6.3.3	Uniform Subwavelength Grating Couplers .....	294
6.3.4	Apodized Subwavelength Grating Couplers .....	295
6.3.5	Polarization-Independent Grating Couplers .....	297
6.3.6	Wideband Grating Couplers .....	297
6.3.7	Focusing Apodized Subwavelength Grating Coupler .....	299
6.3.8	Broadband Focusing Subwavelength Grating Coupler .....	301
6.3.9	Polarization-Insensitive Focusing Subwavelength Grating Coupler .....	302
6.4	Use of SWGs for Waveguide Devices and Mid-IR Photonics ...	304
6.5	Numerical Optimization for the Design of Subwavelength Structures .....	309
6.5.1	Perfectly Vertical Grating Coupler for Multi-core Fiber .....	310
6.5.2	Subwavelength Dual-Polarization Grating Coupler for Few-Mode Fiber .....	312
6.5.3	Dual-Wavelength-Band Focusing Subwavelength Grating Couplers (DWB FSWGCs) .....	315
6.5.4	Hyperuniform Disordered Silicon Photonic (HUDSiP) Polarizers .....	316
6.6	Conclusion .....	317
	References .....	318
7	<b>Non-Hermitian Physics and Engineering in Silicon Photonics</b> .....	323
	Changqing Wang, Zhoutian Fu, and Lan Yang	
7.1	Introduction .....	324
7.2	Non-Hermitian Physics: From Quantum Mechanics to Optics .....	326
7.2.1	Non-Hermitian Physics in Quantum Mechanics .....	326
7.2.2	Paraxial Propagation of Electromagnetic Fields in a Transverse Complex Potential .....	327
7.2.3	Wave Scattering in a Longitudinal Complex Potential .....	329
7.2.4	Non-Hermitian Optical Waveguides and Resonators .....	331
7.3	Spectral Singularity and Enhanced Sensing .....	332
7.3.1	Spectral Singularity at Exceptional Points .....	333
7.3.2	EP-Enhanced Nanoparticle Sensor .....	334
7.3.3	EP-Enhanced Gyroscope .....	336
7.4	Mode Interactions and Lasing Effects .....	338
7.4.1	Chiral Modes at Exceptional Points .....	338

7.4.2	Unidirectional Lasing	339
7.4.3	Single-Mode Lasers	340
7.4.4	Revival of Lasing by Loss	341
7.4.5	Petermann Factor and Laser Linewidth	343
7.4.6	Other Non-Hermitian Lasing Behavior	344
7.5	Scattering Properties and Light Propagation	345
7.5.1	Unidirectional Zero Reflection at Exceptional Points	345
7.5.2	Nonreciprocal Light Transport in Nonlinear Parity-Time Symmetric Systems	347
7.5.3	Electromagnetically Induced Transparency in Non-Hermitian Systems	349
7.6	Topological Features and Mode Switching	351
7.6.1	Dynamics of Encircling EPs	352
7.6.2	Asymmetric Mode Switching	354
7.7	Conclusion and Outlook	356
	References	358
<b>8</b>	<b>Topological Photonics with Microring Lattices</b>	<b>365</b>
	Shirin Afzal, Tyler James Zimmerling, and Vien Van	
8.1	Introduction	365
8.2	Topological Photonic Insulators in 1D Microring Lattices	366
8.2.1	1D Microring Lattice as an SSH Topological Insulator	366
8.2.2	1D Microring Lattice as a Floquet Topological Insulator	372
8.3	Topological Photonic Insulators in 2D Microring Lattices	378
8.3.1	2D Microring Lattices as Chern Insulators	379
8.3.2	2D Microring Lattices as Floquet Insulators	381
8.3.3	Experimental Realization of 2D Floquet Microring Lattices	389
8.4	Conclusion	394
	References	395
<b>9</b>	<b>Parallel Digital Gradient Search Technique for Rapid Automated Alignment of Devices on Silicon Photonics Integrated Circuits</b>	<b>399</b>
	Scott Jordan	
9.1	An Application-Driven Challenge	399
9.2	Photonics to the Rescue: Energy, Speed, Fidelity, Scalability and Sustainability?	400
9.3	Silicon Photonics	401
9.4	The Dinosaur Falls: Extinction of the Loops	403
9.5	Operating Principle	404
9.6	It is 1985 All Over Again: An Ecosystem Rises	405
9.7	Down Deep: Implementing the Parallel Alignment	407

9.7.1	Area Scans	408
9.7.2	Gradient Search	408
9.7.3	Example Case: Array Device Alignment	410
9.8	Alignment Enables the Quantum Era	411
9.9	Conclusion	413
	References	413

**Part III Advances in Computation Schemes**

<b>10</b>	<b>Neuromorphic Silicon Photonics for Artificial Intelligence</b>	<b>417</b>
	Bicky A. Marquez, Chaoran Huang, Paul R. Prucnal, and Bhavin J. Shastri	
10.1	Introduction	417
10.2	Background: Neuroscience and Computation	419
10.2.1	Digital Versus Analog	421
10.2.2	Artificial Neural Networks	423
10.3	Electronics and Photonic Platforms	425
10.3.1	Electronics	425
10.3.2	Photonics	426
10.4	Silicon Photonic Neural Networks	428
10.4.1	MZI-based Processing Unit	429
10.4.2	Photonic Reservoir Computing	433
10.4.3	Broadcast-and-Weight Architecture	435
10.5	Summary and Concluding Remarks	444
	References	445
<b>11</b>	<b>Quantum Processors in Silicon Photonics</b>	<b>449</b>
	Stefano Paesani and Anthony Laing	
11.1	Introduction	449
11.2	Photonic Quantum Information Processing	450
11.2.1	Quantum States of Light	450
11.2.2	Encoding Qubits and Qudits in Photons	451
11.2.3	Processing Photons with Linear Optics	452
11.2.4	Scalable Photonic Quantum Computing Architectures	453
11.3	Silicon Quantum Photonic Technology	454
11.3.1	Integrated Photon Sources	454
11.3.2	Linear-Optical Components	459
11.3.3	Detection Systems	460
11.3.4	Single-Photon Filters	460
11.3.5	Optical and Electronic Packaging	461
11.3.6	Scaling Silicon Quantum Photonic Circuits	461
11.4	Silicon Photonic Quantum Processors	462
11.4.1	Entanglement Generation and Processing in Silicon Photonics	463

11.4.2	High-Dimensional Quantum Entanglement in Silicon .....	465
11.4.3	Measurement-Based Quantum Computing in Silicon Quantum Photonics .....	466
11.4.4	Networking Silicon Quantum Devices .....	467
11.5	Applications for Near-Term Photonic Quantum Processors .....	467
11.5.1	Boson Sampling Machines .....	468
11.5.2	Scaling Boson Sampling with Silicon Quantum Photonics .....	472
11.5.3	Quantum Simulation via Boson Sampling .....	475
11.6	Outlook .....	480
	References .....	480
<b>12</b>	<b>An Open Silicon Photonics Ecosystem for Computercom Applications .....</b>	<b>491</b>
	Marco Fiorentino, Zhihong Huang, Di Liang, Sagi Mathai, M. Ashkan Seyedi, and Raymond G. Beausoleil	
12.1	Introduction .....	491
12.2	Process .....	493
12.3	Design Tools .....	494
12.4	Devices .....	496
12.4.1	Passives .....	496
12.4.2	Active Components .....	499
12.4.3	Lasers .....	500
12.4.4	Detectors .....	502
12.4.5	Packaging .....	503
12.5	Conclusions and Future Work .....	505
	References .....	505
	<b>Index .....</b>	<b>507</b>

# Contributors

**Shirin Afzal** Department of Electrical and Computer Engineering, University of Alberta, Edmonton, AB, Canada

**M. Ashkan Seyedi** Hewlett Packard Laboratories, Milpitas, USA

**Raymond G. Beausoleil** Hewlett Packard Laboratories, Milpitas, USA

**Moritz Brehm** Institute of Semiconductor and Solid State Physics, Johannes Kepler University Linz, Linz, Austria

**D. Buca** Institute of Semiconductor Nanoelectronics, Peter Grünberg Institute 9 (PGI 9) and JARA Fundamentals of Future Information Technologies, Forschungszentrum Jülich, Jülich, Germany

**V. Calvo** Univ. Grenoble Alpes, CEA, IRIG-DePhy, Grenoble, France

**A. Chelnokov** Université Grenoble Alpes, CEA, LETI, Grenoble, France

**Xia Chen** Optoelectronics Research Centre, University of Southampton, Southampton, UK

**Zhenzhou Cheng** School of Precision Instruments and Optoelectronics Engineering, Tianjin University, Tianjin, China

**Kateřina Dohnalová** Institute of Physics, University of Amsterdam, Amsterdam, The Netherlands

**Marco Fiorentino** Hewlett Packard Laboratories, Milpitas, USA

**Zhoutian Fu** Department of Electrical and Systems Engineering, Washington University, St. Louis, MO, USA

**J. M. Hartmann** Université Grenoble Alpes, CEA, LETI, Grenoble, France

**Chaoran Huang** Department of Electrical Engineering, Princeton University, Princeton, NJ, USA

**Zhihong Huang** Hewlett Packard Laboratories, Milpitas, USA



**Z. Ikonc** School of Electronic and Electrical Engineering, Pollard Institute, University of Leeds, Leeds, UK

**Scott Jordan** Physik Instrumente (PI) GmbH & Co., California, USA

**Kateřina Kůsová** Institute of Physics, Czech Academy of Sciences, Prague 6, Czech Republic

**Anthony Laing** Quantum Engineering Technology Labs, H. H. Wills Physics Laboratory, University of Bristol, Bristol, UK;  
Department of Electrical and Electronic Engineering, University of Bristol, Bristol, UK

**Di Liang** Hewlett Packard Laboratories, Milpitas, USA

**David J. Lockwood** Measurement Science and Standards, National Research Council Canada, Ottawa, ON, Canada

**Bicky A. Marquez** Department of Physics, Engineering Physics and Astronomy, Queen's University, Kingston, ON, Canada

**Sagi Mathai** Hewlett Packard Laboratories, Milpitas, USA

**Stefano Paesani** Quantum Engineering Technology Labs, H. H. Wills Physics Laboratory, University of Bristol, Bristol, UK;  
Department of Electrical and Electronic Engineering, University of Bristol, Bristol, UK

**N. Pauc** Univ. Grenoble Alpes, CEA, IRIG-DePhy, Grenoble, France

**Fabio Pezzoli** L-NESS and Dipartimento di Scienza dei Materiali, Università degli Studi di Milano Bicocca, Milan, Italy

**Paul R. Prucnal** Department of Electrical Engineering, Princeton University, Princeton, NJ, USA

**V. Reboud** Université Grenoble Alpes, CEA, LETI, Grenoble, France

**P. Rodriguez** Université Grenoble Alpes, CEA, LETI, Grenoble, France

**Simone Rossi** L-NESS and Dipartimento di Scienza dei Materiali, Università degli Studi di Milano Bicocca, Milan, Italy

**Nelson L. Rowell** Measurement Science and Standards, National Research Council Canada, Ottawa, ON, Canada

**Bhavin J. Shastri** Department of Physics, Engineering Physics and Astronomy, Queen's University, Kingston, ON, Canada

**H. Sigg** Laboratory for Micro- and Nanotechnology, Paul Scherrer Institut, Villigen, Switzerland

**Yeyu Tong** Department of Electronic Engineering, The Chinese University of Hong Kong, Shatin NT, Hong Kong SAR, People's Republic of China

**Hon Ki Tsang** Department of Electronic Engineering, The Chinese University of Hong Kong, Shatin NT, Hong Kong SAR, People's Republic of China

**Vien Van** Department of Electrical and Computer Engineering, University of Alberta, Edmonton, AB, Canada

**Elisa Vitiello** L-NESS and Dipartimento di Scienza dei Materiali, Università degli Studi di Milano Bicocca, Milan, Italy

**Changqing Wang** Department of Electrical and Systems Engineering, Washington University, St. Louis, MO, USA

**Lan Yang** Department of Electrical and Systems Engineering, Washington University, St. Louis, MO, USA

**Wen Zhou** Department of Materials, University of Oxford, Oxford, UK

**Tyler James Zimmerling** Department of Electrical and Computer Engineering, University of Alberta, Edmonton, AB, Canada

**Part I**  
**Advances in Fundamental Research**

# Chapter 1

## Optical Properties of Si Nanocrystals Enhanced by Ligands



Kateřina Dohnalová and Kateřina Kůsová

**Abstract** Compared to bulk silicon, silicon nanocrystals (Si-NCs) show modified properties, such as tunable emission and enhanced radiative rate, as a result of the quantum confinement, surface chemistry and environment. While the effect of quantum confinement is well understood and experimentally confirmed on the hydrogen-capped Si-NCs, the surface effects in Si-NC with other types of ligands can be very complex and hard to predict. In our work, we argue that the surface chemistry, be it ligands and/or shell, can be designed to further improve the radiative rate of the Si-NCs, beyond what is achievable by the quantum confinement alone. Our experimental work shows a number of effects that indicate that in many instances, the core and surface capping cannot be separated, and optical properties cannot be clearly interpreted as “extrinsic” (related to the surface capping agent) or “intrinsic” (related to the core only). To this end, we performed also a detailed theoretical analysis of a number of surface ligands, to identify the role of chemistry and how that improves the optical properties of Si-NCs. Based on these investigations and findings, we realized two main things. Firstly, we argue that one cannot derive a simple rule to predict which type of element or molecule will improve or deteriorate the optical properties, because every individual element added (covalently) to the surface of Si-NC contributes to the electronic density via several mutually dependent effects, such as (i) orbital displacement, (ii) direct contribution of surface species into the density of states close to the bandgap, (iii) charge transfer due to the relative polarity of the surface capping element and Si, or (iv) ligand/matrix induced strain. Secondly, we realized that the **k**-space projections of the molecular orbitals, i.e., the band structure

---

K. Dohnalová (✉)  
Institute of Physics, University of Amsterdam,  
Science Park 904, 1098XH Amsterdam, The Netherlands  
e-mail: [k.newell@uva.nl](mailto:k.newell@uva.nl)

K. Kůsová  
Institute of Physics, Czech Academy of Sciences,  
Cukrovarnická 10, 162 00 Prague 6, Czech Republic  
e-mail: [kusova@fzu.cz](mailto:kusova@fzu.cz)

of the nanocrystal, are an essential and critical tool for investigations of the electronic and optical properties in materials with an originally indirect bandgap, since the surface chemistry in our simulations affects strongly the whole band structure.

## 1.1 Introduction

Silicon is a cornerstone of the modern civilization. Thanks to all its superlatives, such as abundant resources, non-toxicity, bio-compatibility and biodegradability, chemical robustness, low cost production, naturally forming oxide, and many more advantageous properties, it is in fact desirable material for any application. Silicon makes up about 28% of the Earth's crust by mass. Bulk silicon dominates CMOS micro-electronics technologies and enabled digital technologies through transistors to the computing central processing unit (CPU). It also plays an important role in photovoltaics and the detector industry, despite its poor band-edge absorption, for which it compensates by a higher material thickness. Silicon is currently entering also battery applications, for its enormous capacity for Li ion intake [27]. Silicon was reported to be, even in its nanocrystalline form, non-toxic [3, 9, 56, 125] and bio-degradable [154], with superior photo- and pH-stability [82], which opens opportunities also in the traditionally high health risk areas such as cosmetics, agriculture or medicine, for example, as theranostic agents [170]. However, for optical applications in lighting, displays, lasers, and amplifiers, as well as thin film photovoltaics, bulk silicon is not best suited due to its indirect bandgap (Fig. 1.1a). Radiative recombinations of electrons and holes, as well as optical excitations of electrons across the bandgap, require the participation of phonons, which lowers the probability of such transitions. The resulting weak oscillator strength of the optical transitions leads to a low radiative rate and a slow absorption onset with a weak absorption at the band-edge.

Nevertheless, finding/designing a silicon form that can efficiently emit light is obviously highly desirable. A silicon light source would enable the realization of the long awaited on-chip-integrated silicon laser and hence also all-Si photonics (the main topic of this book series), and consequently also optical CPU architecture [1]. Moreover, such a light source could also be implemented in the on-chip integration of the light emitting diodes (LEDs) [146], desired for the light-weight and modular micro-LED displays and lighting. Efficient band-edge absorption would be beneficial for silicon-based thin solar cells, which would also enable a wide spread of solar energy for transportation and other areas where besides efficiency also portability or light-weightiness are essential. Also, because of its non-toxicity and bio-compatibility, silicon can play an essential role in the bio-imaging [56] and bio-integration (with human body) of optically driven micro-devices, sensors, and interfaces [101].

For the last two decades, we have been searching experimentally and theoretically for paths toward enhanced optical capabilities of silicon, especially the wavelength tunability and radiative rate, via combining the quantum confinement and surface

engineering in ligand-capped silicon nanocrystals (Si-NCs) (We note that for simplicity, we use the “Si-NCs” term also for materials, where the crystallinity of the nanoparticle has not been proven or measured and should be better named silicon nanoparticles). Properties induced by the surface chemistry are measured experimentally on both single nanoparticle and ensemble levels. Such analysis is combined with theoretical simulations via semi-empirical tight binding and from first principles by the use of self-consistent ground state density functional theory (DFT).

### 1.1.1 Quantum Confinement

The most reliable route toward an enhanced oscillator strength, and hence also the enhanced radiative rate and absorption cross section, has been so far via the utilization of the quantum confinement in Si-NCs. Bright size-tunable emission from the Si-NCs was first reported in 1990 in a pioneering work of Canham et al. [19] on H- and oxidized porous silicon, followed by many more reports from differently prepared and capped Si nanostructures in the following three decades [8, 26, 29, 33, 43, 67, 78, 107, 140, 143, 144, 150, 179, 185].

Quantum confinement in Si-NCs has a considerable effect on their electronic structure, but only for radii comparable or smaller than the bulk silicon’s excitonic Bohr radius of  $\sim 4.9$  nm. In such a case, strong spatial confinement of carriers results in a shift of valence and conduction bands, leading to a bandgap “opening”, where the bandgap energy increases with the decreasing Si-NC size (Fig. 1.1b, d–g). According to the simplest effective mass approximation (EMA) model, the optical bandgap  $E_g$  scales with the NC diameter  $d$  via an inverse parabolic dependence  $E_g(d) \propto d^{-2}$  as a result of the quantum localization. We also need to add the Coulomb term, which scales with  $\propto d^{-1}$  and small polarization terms [14]. In reality, experimentally investigated Si-NC samples show slightly different values of the exponent, reported in the literature between 1.3 and 2.0 [122, 214]. The bandgap energy determines the photoluminescence (PL) peak from the Si-NCs, which can be tuned in a wide spectral range, from ultraviolet (UV) at  $\sim 260$  nm to near infrared (NIR) at 1100 nm [43, 179] (Fig. 1.1d–g). This broad spectral tunability has been experimentally and theoretically proven in the hydrogen-capped Si-NCs (Fig. 1.1b, d, g) [43]. Despite being an ideal model of an Si-NC for theoretical calculations, H-capped Si-NCs are only rarely studied experimentally due to their increased sensitivity to air and UV light, leading almost immediately to at least partial oxidation, as discussed in more detail below. This is why only a few reports are included in the collection of literature data plotting the experimentally reported PL maxima as a function of NC size, which yields an exponent of 1.33, but shows a low spread of data points around the fitted curve. In Si-NCs with other than H-capping, often a much narrower tunability range is observed [37, 46, 76, 124, 172, 207] due to either a presence of surface sites that act as a traps for the excited carriers [43, 211], or due to the presence of strain [116], or simply as a result of limitations of the preparation procedure. Moreover, chemically

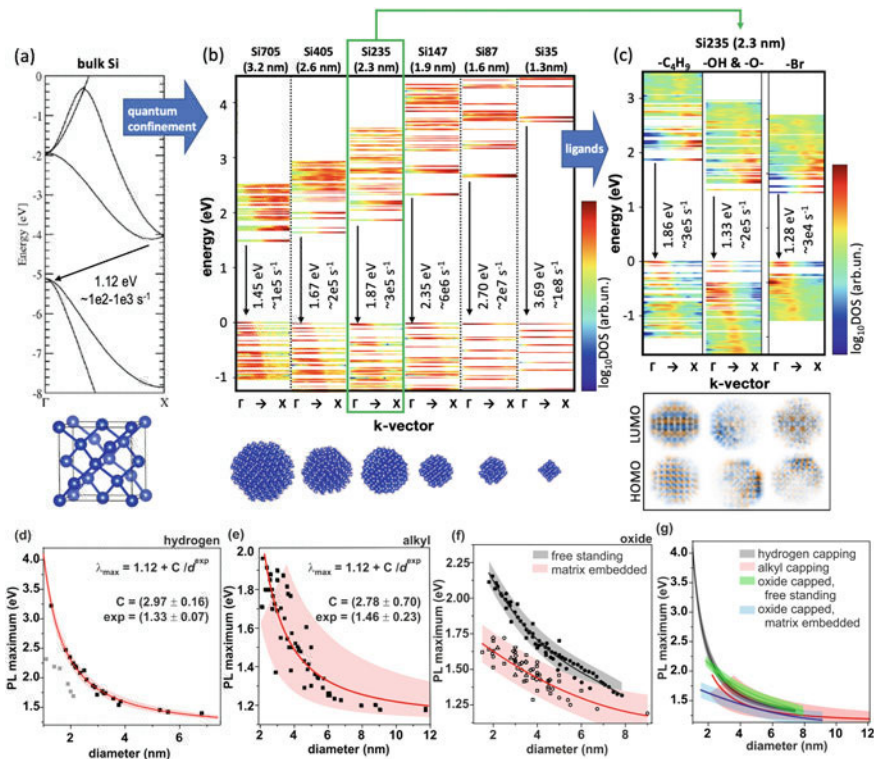


**Fig. 1.1** Quantum confinement effects in Si-NCs. **a** Bulk silicon band structure in the  $\Gamma$ -X direction, critical for the optical properties, where the bandgap can be identified. Bottom panel shows a silicon unit cell with the diamond crystalline structure. **b** k-space resolved density of states (DOS) for the H-capped Si-NCs of diameter from 1.3 to 3.2 nm, simulated by the DFT using cp2k code (full settings are discussed in [44]). Bottom panel shows the relative sizes and shapes of the simulated Si-NCs. **c** "Fuzzy" band structures of 2.3 nm Si-NC capped 50% by hydrogen and 50% by a butyl ligand -C<sub>4</sub>H<sub>9</sub> (left), partly capped with -H and partly oxidized with -OH and -O- bonds (middle) and fully -Br capped surface (right). Below are shown real-space 2D cross sections of the highest occupied molecular orbital (HOMO) and the lowest unoccupied molecular orbital (LUMO) wavefunctions. The color scheme in (b, c) represents the DOS on a log-scale. Bandgap energy and phonon-less thermalized ( $T = 300$  K) radiative rates are given in (b, c) in each respective band structure plot. **d-g** Comparison of photoluminescence (PL) tunability, experimentally reported by various sources: **d** Fully H-capped Si-NCs [45, 65, 211]. The gray data points [180] are possibly influenced by strain and are therefore not included in the fit. **e** Alkyl-capped Si-NCs [68, 79, 85, 96, 145, 162, 175, 207, 214]. **f** Oxidized Si-NCs [116]. Solid symbols in (f) denote Si-NCs prepared as free-standing (e.g., by wet etching or plasma synthesis followed by slow oxidation). Open symbols in (f) stand for matrix-embedded Si-NCs (prepared, e.g., as SiO<sub>x</sub>/Si superlattices or by ion implantation or samples involving thermal oxidation). The fits are meant only as a description of the data and are  $\text{PL max} = -0.0027d^3 + 0.056d^2 - 0.47d + 2.9$  for the free-standing and  $\text{PL max} = 0.0058d^2 - 0.13d + 1.9$  for the matrix-embedded samples. Data from [116] are reused with permission from AIP Publishing. Panels (d-f) contain also fits of the data and the corresponding 95% confidence bands. **g** Comparison of fit curves from panels (d-f)

different surface ligands were themselves experimentally [22] and theoretically [215] shown to cause spectral shifts.

The effects of the quantum confinement on the bandgap energy is common to all types of semiconductor NCs. In an indirect bandgap semiconductor, such as silicon, additional effects occur due to the relaxation of the  $\mathbf{k}$ -selection rule as a consequence of the larger spatial confinement of carriers. In silicon NCs, this in turn enhances the radiative rate  $k_{\text{rad}}$ , based on the theoretical calculations, proportionally to the inverse cubic function  $k_{\text{rad}}(d) \propto d^{-3}$  [8]. In particular, there is about a 3–4 orders of magnitude increased phonon-less radiative rate in the smallest Si-NCs, when compared to the bulk Si, reaching  $\sim 10^7 \text{ s}^{-1}$  for the simulated  $\sim 1 \text{ nm}$  H-capped Si-NCs [39, 44, 75, 159]. Despite such a considerable improvement, radiative rates for the Si-NCs emitting in the visible spectral range still remain much lower than those in the traditionally employed direct bandgap semiconductor NCs with the radiative rates exceeding  $10^8$ – $10^9 \text{ s}^{-1}$ , suggesting a persistently indirect nature of the bandgap in the Si-NCs and the importance of the  $k$ -space information in general.

An interesting development with respect to the enhanced radiative rate in Si-NCs has been published only very recently [180]; The authors study a series of H-capped Si-NCs prepared by a standard bottom-up sol-gel approach and observe a gradual size-induced PL shift from 700 to 530 nm. Whereas the larger Si-NCs exhibit the typical slow PL decay rates, at the size range below 1.7 nm, the PL decay rate is enhanced by about five orders of magnitude. (Argumentation is provided as to whether this PL decay rate is most likely the radiative rate.) This observation could be interpreted as the switch between indirect bandgap-like and direct bandgap-like emission in Si-NCs; the authors interpret their experimental data in terms of a switch between a bulk-like and molecular size regime. It is unknown why these particular very small Si-NCs exhibit fast PL decay, but the authors admit to the possibility that the small Si-NCs are strained.

Despite the generally limited success in the enhancement of the radiative rate for Si-NCs with emission in a visible spectral range and often observed limited tunability range of the bandgap in various ligand-capped Si-NCs, some of the best Si-NC materials with bright emission have already been implemented in various optoelectronic prototypes of light emitting devices [6, 43, 51, 55, 139, 163]. Nevertheless, such devices have not yet been commercialized and remain in a research and development stage, suggestive of the fact that a much needed improvement of their optical properties is still required.

### 1.1.2 Complex Role of Surface Chemistry

The most frequently quoted property of a nanocrystalline semiconductor material is the above discussed “size-effect”. One of its manifestations is the optical bandgap tunability via quantum confinement in the NCs smaller than the Bohr’s excitonic radius. In most semiconductor NCs, such as the direct bandgap III–V or II–VI NCs, the size of the core offers a robust parametrization for the optical bandgap energy.



However, in the case of the Si-NCs, the size of the NC core is not enough to determine neither the optical bandgap energy nor the radiative rate, both being significantly affected by the surface chemistry, e.g., by organic coatings (Fig. 1.1e), oxide capping and strain (Fig. 1.1f).

The often observed strong influence of ligands on the optical properties of the Si-NCs is due to a complex interplay between the core and the covalent surface chemistry with other elements, and the relatively large percentage of atoms being located at the surface (a very useful tool giving insight into the basic possible arrangements of atoms and bonds can be found in [105]). This interplay manifests via charge transfer, strain, orbital displacement, and the direct contribution of the surface elements to the density of states near the bandgap. Silicon is a light element, and its valence electron states are relatively close to the elements that are often considered as capping agents, such as oxygen, nitrogen, or carbon. Silicon can covalently bond with many elements with a various degree of electron sharing/transfer, stability, opto-chemical robustness or resistance against oxidation (which is a strongly preferred reaction under normal conditions). The most robust and studied types of cappings in the literature are H-, silica oxide (O-), hydrocarbon (organic) C-, O- or N-linked ligands, and halides (-Cl, -Br, -I or -F), together with the P- and B- surface co-doped Si-NCs [182]. For the sake of completeness, we note that it is important to realize that the photo-chemical stability of a certain bond cannot be easily deduced from the Si-X bond dissociation energy (DE), derived for the diatomic species [132], because the covalent bond strength changes in the presence of other bonded species, or under strains [202]. This is a result of the different orbital displacement caused by the additional bonded species, which can weaken the bond. Hence, the silane SiH<sub>4</sub> molecule is extremely unstable, violently reacting with oxygen, but Si-NC capped with H can resist oxidation for a very long time. This is because the dissociation of the Si-H bond is easier when in the -Si-H<sub>2</sub> or even -Si-H<sub>3</sub> form, and therefore, the -SiX<sub>3</sub> species on the Si-NC surface are less stable than the -SiX species. Also, various facets on the Si-NC surface have different Si coordination and are therefore subject to different strains in the presence of ligands due to steric hindrance effects. The highly curved surface of small Si-NCs also results in distorted/strained bonds, which further decreases their stability and makes them more prone to reactions or disintegration. For these reasons, stability of, e.g., H-capping on the surface of a Si-NC will differ for a crystalline and an amorphous Si-NC, as well as for large or small Si-NCs, and possibly also for Si-NCs prepared by different methods. This further complicates the main question of this chapter on *how a certain element or molecule influences the optical properties of a Si-NC*, because one type of ligand can lead to very different results, when placed in different positions on the Si-NC surface.

The H-capping is the simplest and best understood ligand, and as such is also a great “clean” starting point for the subsequent surface treatments [149]. Despite the extreme reactivity of the SiH<sub>4</sub> with air, as discussed above, the H-terminated Si surfaces are on their own chemically very stable, because the Si-H bond is strong and nonpolar; however, a direct photo-desorption occurs under a UV-blue irradiation [104]. As a result of the native indirect bandgap, persisting also in small Si-NCs [80, 159], Si-NCs absorb efficiently only from the blue-UV range, rendering the H-

capped Si-NCs surfaces photo-chemically unstable for the light-related applications. Nevertheless, despite their opto-chemical instability, H-capped Si-NCs are often presented in the literature as a reference material and a starting point for theoretical simulations, because their optical properties are purely core-driven.

### 1.1.2.1 Oxide Capping

Silica oxide is naturally forming on the surface of silicon under exposure to air. Therefore, silica oxide-capped Si-NCs are one of the most accessible and analyzed types of Si-NCs. Capping with oxygen atoms can be done in several ways, as a double bond Si=O, as a bridging bond Si-O-Si, or via -OH groups [25]. The first two types have been reported to lead to limited bandgap tunability [74, 166, 167, 200, 211, 216] and slower radiative rates [40, 78]. The limiting effect of oxidation on spectral tunability has been first experimentally reported by Wolkin et al. [211] on porous silicon, prepared from bulk crystalline silicon by electro-chemical etching in solution composed of ethanol, water, and HF acid. This resulted in a H-passivated “nano-sponge” surface [83, 211], which contained small H-capped Si-NCs. As demonstrated by Wolkin et al. [211], the H-capped surface oxidized under exposure to air, when excited by UV light, which was accompanied by a change in color of the emitted PL.

For the larger oxide-capped Si-NCs, the PL peak was shown to be size tunable [10, 23, 52, 84, 122, 187, 211]; however, the tunability would often end in the red range close to 620–650 nm, indicating possible involvement of the surface oxide states [133]. This PL is always characterized by a slow  $\sim \mu\text{s}$  decay, for which it has been named in literature as an “S-band” [17]. For the smaller Si-NCs, the limit to which the emission can be tuned varies greatly through the literature [46]. A detailed overview can be found in [116] with the data sets re-plotted in Fig. 1.1f, clearly illustrating the existence of two distinct classes of oxide-capped Si-NCs, characterized by a different size dependence of the PL maximum. These two classes of Si-NCs correlate with the way the samples were prepared—either as “free-standing” (e.g., by a wet etching) or as “matrix-embedded” (e.g., by an ion implantation). We have hypothesized that in the matrix-embedded samples, the matrix exerts a compressive strain on the crystalline Si-NC cores, which leads to the corresponding shift in the electronic bands and consequently to the reported red-shifted emission, when compared to the free-standing oxidized Si-NCs. Interestingly, an analogical influence of the matrix was also reported in  $\text{CdS}_x\text{Se}_{1-x}$  NCs [176]. An opposite effect, i.e., the expansion of the crystalline lattice in oxidized Si-NCs, was demonstrated by doping Si-NCs with lithium [102], leading to a blue-shifted PL emission. Interestingly, the collection of the experimental data on the PL peak maximum as a function of the size of the NC  $d$  from the literature in Fig. 1.1f could not be satisfactorily fitted using the EMA-like model  $E_g^{\text{NC}} = E_g^{\text{bulk}} + C/d^{\text{exp}}$ . Therefore, a polynomial, meant simply as a quantitative description, was used. The different shape of the size dependence of the bandgap might imply that an additional effect of possibly size-dependent strain is present in such oxidized samples. These oxide-capped Si-NCs exhibit typical stretched-exponential PL decay of the order of tens or hundreds of microseconds

[72], whose various properties [81, 197], including (the lack of) saturation of its power dependence [36, 73], were discussed in countless publications.

Interestingly, unlike other types of capping, a thin oxide shell was shown to lead to a very narrow luminescence linewidth [183], which could be very beneficial, for example, a high color definition required in application for displays. Oxidized Si-NCs can be also very interesting for application in the medical field. They are relatively photo-stable and were shown to be non-toxic [98, 155, 170, 177, 193]. In aqueous environments, oxide-capped Si-NCs slowly dissolve into the omnipresent, benign silicic acid [155], i.e., they are bio-degradable. The size of the luminescent oxide-capped Si-NCs is always below  $\sim 5$  nm, which is a limit for a safe excretion from a living organism via urine [126], but can be an issue for its possible entry through the blood-brain barrier [71]. Also, upon excitation, oxide-capped Si-NCs are a source of oxygen radicals that are toxic to the neighboring tissue, an effect suggested for possible use in photo-induced local cancer treatment [108, 156, 191], or as a carrier of radioactive isotopes [158]. The red and slow decaying emission offers also a great contrast to the often fast decaying blue-green emission from organic tissue [144]. For the optical applications, however, the oxidation of the Si-NC surface might not be desired, when a full spectral tunability through the whole visible range is required, as well as high radiative rates.

### 1.1.2.2 Organic Capping

Another type of surface capping, well represented in the literature, but less understood theoretically, is via organic molecules, often long alkyl chains attached via hydrosilylation. Unlike in oxidized Si-NCs, the bandgap tunability curve for alkyl-capped SiNCs (Fig. 1.1e) can be fitted with an EMA-like model, albeit using a slightly different exponent than that in H-capped Si-NCs. Thus, this shape of the tunability curve suggests that in the alkyl-capped Si-NCs, the emitted PL resembles more that of the “ideal” H-capped Si-NCs system rather than the PL of the oxidized Si-NCs, in agreement with ab-initio studies [44, 171]. The large spread of the reported data around the fitted curve in Fig. 1.1e, also critically pointed out in [85] for this type of Si-NCs, is partly a result of the inclusion of many reports in this data set, where every measurement, especially the determination of size, is inevitably connected with an error [189, 190]. However, as some recent literature suggests, it can also signify some degree of influence of the alkyl chains on the emitted PL, be it their length, type of attachment or surface coverage [44]. Furthermore, synthesis of organically capped Si-NCs often involves heating of organic solvents, which has been reported to lead to the presence of other than Si-NC emitters, such as e.g. carbon dots, which could skew the reported PL properties if not carefully eliminated [17, 151, 209].

The comparison of the PL tunability curves in Fig. 1.1g confirms the presence of a limit around the end of the red spectral range for most of the experimentally investigated Si-NCs (except the H-capped ones) [37, 76, 180, 207]. It is very likely that most of the experimentally investigated organically capped Si-NCs are partly oxidized under UV-blue illumination, since due to the steric hindrance between the

organic ligands, the surface cannot be 100% capped by organic molecules [44]. A possible culprit of the observed difference in the tunability limit of alkyl- and oxide-capped Si-NCs with respect to the H-capped ones might also be a “stability problem”, where the surface of a too small Si-NC might be too reactive to be passivated after the core has been formed, since the attachment of ligands can simply lead to the disintegration of the whole Si-NC. Such a stability problem could in principle be circumvented by the various one-pot synthesis schemes of already-passivated Si-NCs [165].

The PL decay is for the larger, red-NIR emitting alkyl-capped Si-NCs, similarly slow as for the oxide-capped Si-NCs, albeit with much better quantum yields [85, 97, 175]. Moreover, there are certainly some new developments in this field of research: Ensemble-induced effects start to be discussed in these Si-NCs [92, 145], the discussion on the periodicity of the core and its influence on the PL has been opened [189, 190], and even a fast PL component has been reported within this red emission band [11]. Pressure-dependent PL studies of organically capped Si-NCs perfectly agree with bulk-like band shifts [79], pointing toward a possible core-related origin. Interestingly, very similar band shifts were reported also in oxide-capped Si-NCs [116]. Comparable PL changes in alkyl- and oxide-capped Si-NCs were also reported in temperature-resolved measurements [138]. On the contrary, alkyl- and oxide-capped SiNCs were observed to exhibit different phonon modes in Raman measurements [86], interpreted in terms of oxide-induced strain.

While origin of the slow decaying PL in organically capped Si-NCs is accepted as core-related, the vast majority of the bottom-up wet-chemically synthesized Si-NCs exhibit unusually fast, nanosecond decaying PL in the blue-green spectral range [41, 53, 85, 113, 173, 206, 210, 217], whose origin is still a subject of intense debate and will be discussed in the following sections.

### 1.1.2.3 Direct Bandgap-Like Emission from Si-NCs: The “F-Band”

Quite controversially, a bright emission with direct bandgap-like radiative rates of  $10^7$ – $10^9$  s<sup>-1</sup>, and often a blue-green spectrum, has been reported experimentally from various Si-NCs capped with oxide [5, 90, 109] (see the latest review in [17]), and also for organic ligands [41, 53, 85, 113, 173, 206, 210, 217]. Throughout the literature, to differentiate between the traditionally slow decaying Si emission and the often observed fast decaying emission bands, the two are often labeled as the “S-band” for the slow emission and the “F-band” for the fast one. The “S-band” PL has typically 1–100s microsecond lifetime and red-NIR tunable energy, as described above. The “F-band” is very often confined to the blue-green spectral region and has a fast 1–10 nanosecond PL decay. In the past, the “F-band” has been assigned mostly to an extrinsic origin, such as oxygen- [12, 58, 59, 66, 69, 77, 168, 192, 194, 212] or nitrogen-related surface sites [34]. Other literature sources gave evidence for its possible intrinsic origin [42, 99, 152, 164, 195, 205] connected with the core or a combination of intrinsic and surface-related emissive sites [30, 44, 64]. A large body of literature explores also the possibility that this emission is entirely unrelated

to the Si-NCs and is caused by carbon dots or other organic impurities [18, 20, 21, 24, 35, 57, 121, 129, 130, 151, 201, 209]. With respect to the carbon impurities, in our recent critical study [209], we show that despite the confirmed presence of Si and NCs in the elemental and materials analysis of the sample, the emission still did not originate from the Si-NC, but from ill-defined organic impurities, possibly carbon dots. Hence, one must perform synthesis of a control sample, as well as a direct (preferably correlative) single-dot microscopy, to be able to confirm that the emissive nanoparticle is indeed the Si-NC, and not a carbon dot, which would also exhibit size-dependent properties.

At least some blue PL can be emitted by nearly any (mostly organic or oxide-related) compound, when detected with high enough sensitivity. Therefore, clearly, extreme care needs to be taken to rule out other species than Si-NCs as the source of the observed PL. However, if we exclude the possibility of an erroneous assignment, given the broad scope of the reported origins of the fast emission, it is highly improbable that a single, all-encompassing explanation exists. More probably, different physical phenomena are responsible for the fast emission in the different samples, and often, more than one of the proposed mechanisms might apply even in a single sample. Thus, we do not believe that the F-band label should apply to such a broad scope of phenomena and that several, possibly overlapping, sub-groups exist within this type of emission, as we have already suggested elsewhere [117]. Therefore, a detailed preparation history of any studied sample needs to be complemented by a thorough characterization to differentiate between the individual modes of emission. Additionally, taking into account the very small size of just a few crystallographic planes, sometimes even the concepts of, e.g., a “surface-site” might not be that easy to grasp. In most cases, the wavefunction of an electron or a hole inside a NC will be spread over a large part of the core [44], rather than just residing on a certain surface site or being homogeneously delocalized over the whole core volume. Such an effect is evident, e.g., from the real-space localization of the highest occupied molecular orbital (HOMO) and the lowest unoccupied MO (LUMO) wavefunctions in, e.g., Fig. 1.1c. Therefore, except for few extreme cases, a differentiation between a surface- or core-related origin can be blurred [110]. In fact, the reality of the light emission of the Si-NC is governed by a complex interplay of many intertwined phenomena, as we have recently discussed in [44], and parallel experimental and theoretical approaches are “a must” in order to achieve further progress.

Despite the described uncertainties, the silicon community is dedicated to uncover the origin of this fast decaying and often very efficient “F-band” emission, as it holds great promises for optical applications of silicon. In our experimental work, we researched the “F-band” emission using various methods and differently prepared Si-NCs, including reports of positive optical gain [49]. In our most recent work, we focus on the  $\mathbf{k}$ -space projected density of states of Si-NCs with various ligands [48, 80, 115, 159], described in the following section, to uncover the possible evolution of the “direct bandgap-like” optical transitions that could stand behind the F-band emission.

### 1.1.3 The *K*-Space Projections of the Density of States

The physics of emission from the Si-NCs is in general challenging and not yet fully controlled due to a complex, almost organic-like covalent chemistry on the silicon surfaces [16], which can, moreover, depend also on the preparation technique of the Si-NC core [208]. This leads to a complex electronic interplay between the silicon and ligand states, where the surface bonded elements can strongly affect the whole electronic structure of the Si-NCs [44] (Fig. 1.1c), especially the real- and *k*-space density of states (DOS) profiles, and consequently also the bandgaps and radiative rates. In fact, the *k*-space resolved DOS in NCs is under-represented in most of the available theoretical literature and is not a standard option in the DFT simulations packages (unlike for bulk crystals). However, this might be slowly changing, as more recent work is adopting this approach as well [11, 162].

Band structure, or a *k*-space projected DOS, is a very useful formalism for the description of the electronic and optical properties in bulk crystalline materials. This often used approximation uses a simplified description of a quantum state of a solid based on single electron states. It assumes that the electrons travel in a static potential without dynamically interacting with the lattice vibrations, other electrons, etc., (or in other words the adiabatic and Hartree–Fock approximations are applied to the corresponding Schrödinger equation). This approach has proven very successful even beyond the scope of the initial approximation, as, for example, an exciton or a dopant/ impurity/ defect can be viewed as a small correction to the states within the band structure. One important assumption from which the band structure concept is derived is the requirement for a long-range translational symmetry in an ideally infinite crystalline material. In a macroscopic crystal, the lattice can be considered infinite without too much simplification, since 1 cm<sup>3</sup> of a crystalline material can contain some 10<sup>23</sup> atoms. Similar simplification, however, would be far too crude for a small nanocrystal, whose crystalline core can contain as few as 500 atoms. Despite clearly breaking the requirement for being infinite and having a long-range translational symmetry, the band structure description has been used by the experimentalists to qualitatively and sometimes quantitatively describe some of the aspects of the behavior of semiconductor nanocrystals [60, 89].

In our tight binding simulations [48], we adopted this approach for the highest occupied molecular orbital (HOMO) and lowest unoccupied molecular orbital (LUMO) (see Supplementary information in [48]; Fig. 1.2a). To uncover the *k*-space profile of the density of states  $|\Psi_i(\mathbf{k})|^2$ , we performed a Fourier transform of the real-space molecular orbital  $|\Psi_i(\mathbf{r})|$ . The density of states  $\rho_i\mathbf{k} = |\Psi_i\mathbf{r}|^2$  can be then plotted along a specific direction, e.g.,  $\Gamma$ –X and  $\Gamma$ –L. This allowed us to identify an enhancement in the DOS around the  $\Gamma$  point for the LUMO, indicating direct bandgap-like transitions. This finding was accompanied by a 1000× enhancement in the phonon-less radiative rates and enhanced absorption cross section (Supplementary information in [48]).